X-Ray Diffraction Studies on the Structure of the Tri- and Tetrathiocyanatomanganate(II) Complexes and Solvated Lithium Ion in *N,N*-Dimethylformamide

Tamás RADNAI,† Shin-ichi ISHIGURO,†† and Hitoshi OHTAKI*
Coordination Chemistry Laboratories, Institute for Molecular Science, Myodaiji-cho, Okazaki 444
†† Department of Electronic Chemistry, Tokyo Institute of Technology at Nagatsuta, 4259 Nagatsuta, Midori-ku, Yokohama 227
(Received January 16, 1992)

The structure of the tri- and tetrathiocyanato-*N*-manganate(II) complexes in *N,N*-dimethylformamide (DMF) solution was determined by the solution X-ray diffraction method at 25 °C. The most probable structure of the tri-complex is octahedral with additional three DMF molecules in the first coordination sphere, while the tetra-complex is tetrahedral. The Mn–O and Mn–N bond lengths were determined to be 220 pm in both complexes. The structure of the octahedrally solvated lithium ion $[Li(dmf)_6]^+$ with the Li–O bond length of 195 ppm was also determined in an LiSCN solution of DMF.

Recently the thiocyanate ion in solution has attracted much attention of coordination chemists because of its ambient nature depending on the properties of the central metal ions and solvent molecules. It is well known that thiocyanate ions can bind to Hg^{2+} through the S atom in water[1] and dimethyl sulfoxide (DMSO)[2] solutions. On the contrary, the binding atom is N for Zn^{2+} in these solutions.[1,2] For Cd^{2+} which has a Lewis acidity between Zn^{2+} and Hg^{2+}, both N and S atoms bind to Cd^{2+} and the tetrathiocyanatocadmate(II) complex has the structure of $[Cd(NCS)_2(SCN)_2]^{2-}$ in water,[1] while it has the structure of $[Cd(NCS)_3(SCN)]^{2-}$ in *N,N*-dimethylformamide (DMF).[3]

A change from the octahedral to the tetrahedral structure of thiocyanato complexes has often been observed as a function of the ligand number of complexes. However, in most cases the step where the structural change occurs is not well known, although some indications have been obtained on various complexes in aqueous and nonaqueous solvents.

Recent calorimetric and spectrophotometric studies on the thiocyanato-*N* complexes of manganese(II), cobalt(II), and nickel(II) ions suggested the presence of different forms of the thiocyanato complexes in DMF, although all these ions have the similar octahedral solvate structure.[4] For example, the $[Co(NCS)_n(dmf)_{6-n}]^{(2-n)+}$ complexes are octahedral at $n=1$ and 2, while the tri- and tetra-complexes are tetrahedral. For the nickel(II) complexes with thiocyanato ions, no structural change has been suggested over the range of the ligand number from 1 to 4.

According to calorimetric measurements,[4] the structural change from octahedral to tetrahedral has been expected to occur either at the formation of the tri-complex or the tetra-complex in case of manganese(II) ion in DMF:

$$[Mn(NCS)_2(dmf)_4] + NCS^- = [Mn(NCS)_3(dmf)_3]^- + dmf, \quad (1)$$

or

$$[Mn(NCS)_2(dmf)_4] + NCS^- = [Mn(NCS)_3(dmf)]^- + 3dmf, \quad (2)$$

where $[Mn(NCS)_3(dmf)]^-$ indicates a tetrahedral complex, while the other formulae mean that they are octahedral. The calorimetric data suggested a possible equilibrium between the octahedral and tetrahedral trithiocyanatomanganese(II) complexes. No spectroscopic evidence has been obtained so far on this matter.

In the present study we intended to investigate the structure of the tetrathiocyanatomanganate(II) complex by the solution X-ray diffraction method. However, since the presence of the tri-complex could not be avoided in the studied solution, the structural determination was extended to the tri-complex as well.

As far as solvation of lithium ions in DMF solutions is concerned, no reliable structural study is available in the literature. A study by electron diffraction and Raman spectroscopic methods on the complex formation between zinc(II) and bromide ions in DMF in the presence of Li^+ ions led to a qualitative conclusion that Li^+ ions are strongly solvated with DMF molecules.[5] Since we added a large amount of lithium ions in the manganese(II) thiocyanate solution of DMF to produce the tetrathiocyanatomanganate(II) complex, we carried out a structural study on the solvated lithium ion in DMF, too.

The solvation structure of the free thiocyanate ion was also discussed, although solvation of the anion was very weak.

Experimental

Preparation and Analysis of Sample Solutions. All chemicals used were of reagent grade. Two test solutions were

† On leave from: Central Research Institute for Chemistry of the Hungarian Academy of Sciences, Budapest, P. O. Box 17, H-1525, Hungary.

prepared. *Solution A* was a sample in which the same concentration of Li^+ as that in *Solution B* was contained, but no manganese(II) thiocyanate was present. *Solution A* was used for the study of the solvation structure of the lithium ion, as well as that of the thiocyanate ion. In *Solution B*, 0.382 mol dm^{-3} Mn^{2+}, 1.286 mol dm^{-3} Li^+, and 2.050 mol dm^{-3}, NCS^- ions were contained. Considering the stability constants reported for the thiocyanato complexes of manganese(II),[4] we estimated the composition of *Solution B* to contain 70±10% tetra-, 25±10% tri-, and ca. 5% dithiocyanato complexes.

Manganese(II) thiocyanate was prepared by mixing an aqueous solution of manganese(II) sulfate with an excess amount of barium thiocyanate, and then 5 v/v% sulfuric acid solution was added until no more precipitates of $BaSO_4$ were detected. The precipitated $BaSO_4$ was removed by filtration twice through Celite. Manganese(II) thiocyanate thus prepared was recrystallized twice from methanol, washed in ether, dried in vacuum oven and the yielded yellowish crystals were kept in a dry box for further use.

Lithium thiocyanate was recrystallized from a solution after lithium sulfate had been reacted with barium thiocyanate and barium sulfate precipitates had been removed. The highly hygroscopic lithium thiocyanate crystals were very slowly dried in vacuum oven at about 60 °C, and then were completely dried in a desiccator over P_2O_5.

The test solutions *A* and *B* were prepared in a dry box by dissolving the required amounts of sample crystals in twice distilled DMF. The concentration of manganese(II) ions was determined by EDTA titration. Densities of the solutions were determined by using a pycnometer. Compositions, densities, and the stoichiometric volumes of the solutions are given in Table 1.

X-Ray Scattering Measurements. X-Ray scattering measurements were performed at 25 °C with a JEOL θ-θ diffractometer by using Mo $K\alpha$ radiation (λ=71.07 pm). The observed range of scattering angle (2θ) was from 1.5° to 140°. Times required to accumulate 100000 counts at each angle were recorded. Scattered intensities lower than θ=0.75° (s=0.002 pm^{-1}) were extrapolated towards zero at θ=0°. The method of measurements and data treatments were essentially the same as for pure DMF.[6,7]

Table 1. The Composition (mol dm^{-3}), Stoichiometric Ratios of the Components, Densities, and Stoichiometric Volumes, V, in *Solutions A* and *B*. The Stoichiometric Volume is Defined to Contain One Lithium and One Manganese Atom in *Solutions A* and *B*, Respectively

	Solution A	*Solution B*
Mn	—	0.382
Li	1.286	1.286
S	1.286	2.050
C	38.555	37.995
N	13.709	14.032
O	12.423	11.982
H	86.960	83.870
NCS:Mn	—	5.369
NCS:Li	1.000	1.594
DMF:Mn	—	31.373
DMF:Li	9.656	9.313
Density/g cm^{-3}	0.992	1.025
$V/10^{-24}$ cm^3	10.772	10.957

Results and Discussion

Method of Structural Analysis. The observed structure functions $s \cdot i(s)$, wheighted by the modification function $M(s)$ defined by Eq. 3,

$$M(s) = \frac{\sum n_i f_i(0)^2}{\sum n_i f_i(s)^2} \cdot \exp(-ks^2) \quad (3)$$

are shown in Fig. 1, where n_i stands for the number of atom i in the stoichiometric volume, $f_i(0)$ and $f_i(s)$ denote the scattering factors of atom i at s=0 and s, respectively. The damping factor k was chosen as 100 pm^2 in the present case. The radial distribution functions $D(r)$ were derived from the structure functions by Fourier transformation. Pair-correlation functions, $G(r)$ obtained for *Solutions A* and *B* are shown in Figs. 2 and 3, respectively. A first approach for obtaining approximate values of the structural parameters of the expected species in the solutions was carried out from peak shape analysis of the radial distribution functions by using models of the species, and then the results were refined by the non-linear least-squares (LSQ) method. The fit was monitored through the R-factor as defined by

$$R = \frac{\sum[s \cdot i(s)_{exp} - s \cdot i(s)_{model}]^2}{\sum[s \cdot i(s)_{exp}]^2}, \quad (4)$$

where $s=(4\pi/\lambda)\sin\theta$.

The structural analysis of the complexes and solvated ions was carried out in the following way.

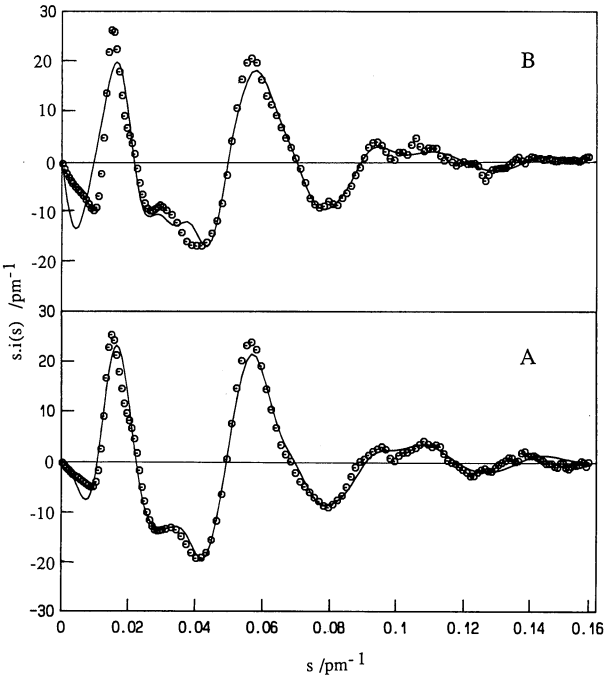

Fig. 1. Experimental (circles) and calculated (full lines) values of the structure functions of *Solutions A* and *B*.

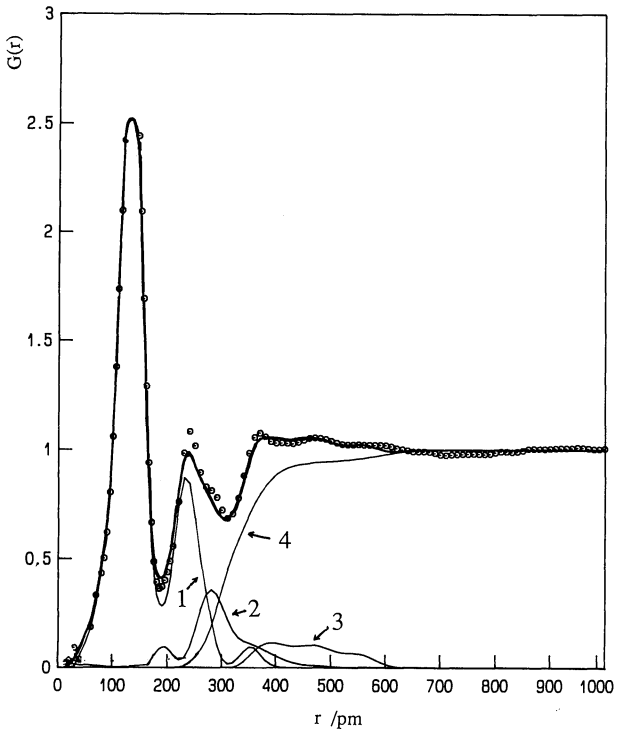

Fig. 2. Pair correlation functions of *Solution A*. Experimental (circles) and theoretical (thick full line, not numbered) values are given together with the intramolecular contributions from DMF molecules and thiocyanate ions (curve 1), solvated Li^+ ions (curve 2), solvated NCS^- ions (curve 3), and from the continuum part of the solution (curve 4).

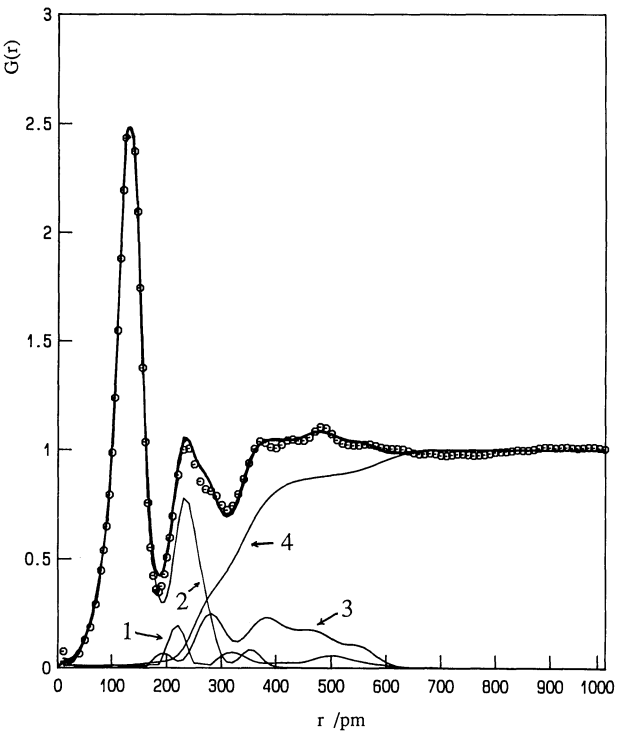

Fig. 3. Pair correlation functions of *Solution B*. Experimental (circles) and theoretical (thick full line, not numbered) values are given together with contributions from intermolecular interactions in the 50 : 50% mixture of $[Mn(NCS)_4]^{2-}$ and $[Mn(NCS)_3(dmf)_3]^-$ complexes (curve 1), intramolecular contributions from DMF molecules and thiocyanate ions (curve 2), solvated Li^+ ions (curve 3), and the continuum part of the solution (curve 4).

(a) The structure function $s\cdot i(s)$ was divided into two parts:

$$s\cdot i(s) = s\cdot i_d(s) + s\cdot i_c(s), \quad (5)$$

where $s\cdot i_d(s)$ represents the structure function arising from the discrete part of the contribution of the interatomic interactions,

$$s\cdot i_d(s) = s\sum\sum n_{pq}c_{pq}j_0(sr_{pq}) \exp(-b_{pq}s^2), \quad (6)$$

and $s\cdot i_c(s)$ describes that from the continuum part,

$$s\cdot i_c(s) = -4\pi\rho_0\sum\sum c_{pq}R_{pq}^2 j_1(sr_{pq}) \exp(-B_{pq}s^2). \quad (7)$$

Here c_{pq} refers to the weight of the contribution of a p–q pair to the total intensities comprising the scattering powers of atoms and their stoichiometric weights, $j_m(x)$ is the spherical Bessel-function of the mth order. The structural parameters describing the discrete terms are the frequency factor n_{pq}, the mean interatomic distance r_{pq} and the temperature factor b_{pq} for the p–q atom pair. For long range interactions beyond the discrete distributions of the distances, the $s\cdot i_c(s)$ term of a continuous distribution of electrons was introduced in order to reproduce the experimental structure functions over the whole experimental range. The included structural parameters are the distance R_{pq} beyond which a continuous distribution of atoms of type q around the p type atom at the center is assumed, and B_{pq} is a parameter describing the sharpness of the boundary at R_{pq}.

The contributions to the structure of each solution can be divided into four parts: (i) the intramolecular structure of the thiocyanate ions and DMF molecules, (ii) the intramolecular structure of the complexes, (iii) the solvation structures around the cations and anions, and (iv) the bulk structure of the solvent. Contributions from long range interactions were included in the continuum part of the structure function.

(b) The intramolecular part of the discrete structural parameters was calculated from the molecular structures of NCS^- [1,3] and DMF[6,7] given in the literature. The same parameters were used for the estimation of intramolecular contributions of the species both in *Solutions A* and *B*.

(c) The range of s from 0.006 to 0.05 pm^{-1} was used for fitting the parameters for the continuum of *Solution A*.

(d) By fixing the intramolecular and continuum parameters, the calculated contributions were subtracted from the total $s \cdot i(s)$ function of *Solution A* to obtain the difference structure function $s \cdot i(s)_{diff}$. Various models were examined for determining the structure of the solvated Li^+ ion as well as that of NCS^- ions to obtain the best fit result to the difference structure function.

(e) The models adopted in the above considerations were tested by using the LSQ method against the total structure function $s \cdot i(s)$. The LSQ fitting procedure was extended over a range of s from 0.002 to 0.165 pm^{-1}.

(f) Similar procedures were applied to the structure function of *Solution B* by assuming that the intramolecular parameters of free thiocyanate ions, and the structure parameters of bulk DMF and solvated lithium and thiocyanate ions remained unchanged from those of *Solution A* upon addition of manganese(II) ions. Then, parameters for the interactions within the manganese(II) complexes of thiocyanate ions were optimized by the LSQ procedure. Several combinations for possible complexes were tested as it will be described below in detail.

The structure functions finally obtained by using the parameter values given in Tables 2 and 3 are shown in Fig. 1 by the full lines for both solutions. The corresponding pair-correlation functions $G(r)$ are shown by the full thick lines (not numbered) in Figs. 2 and 3, together with those of the individual species.

Intramolecular Structure of DMF. An assumption was made that the average intramolecular structure of DMF molecules in the pure state was kept unchanged in *Solutions A* and *B*, and the parameter values for the intermolecular structure of DMF molecules were taken from the literature.[7] The parameter values were even allowed to vary in the fitting procedure, but no significant change could be observed in the result.

Since DMF molecules are practically randomly distributed in the pure state,[6] the assumption of the continuous distribution of electrons was acceptable for the interpretation of the long range intermolecular interactions among DMF molecules. Thus, the intra- and intermolecular interaction parameters were fixed at the literature values during the structural analysis of the solutions. The calculated intermolecular contribution of DMF molecules to the pair-correlation function of *Solution A* is contained in curve 1 of Fig. 2.

Intramolecular Structure of the Thiocyanate Ion. The thiocyanate ion is linear, and the interatomic bond lengths and their temperature factors in solution[1,3] and in crystal[8,9] have been reported in the literature. In the present work we adopted the following values: $r_{C\text{-}N}$=120, $r_{C\text{-}S}$=165, and $r_{S\cdots N}$=280 pm, and $b_{C\text{-}N}$=0.4×10², $b_{C\text{-}S}$=0.4×10², and $b_{S\cdots N}$=1.0×10² pm^2.[1] No further refinement of the values was done in the course of the data treatment.

The sum of the calculated intermolecular contribution of DMF molecules and thiocyanate ions to the pair-correlation function of *Solution A* is shown as curve 1 of Fig. 2.

Solvation of the Lithium Ion. Two models, (i) the tetrahedral and (ii) octahedral structures, for the solvated lithium ions were tested for the residual $s \cdot i(s)$ curve of *Solution A* after subtraction of intra- and intermolecular interactions of DMF molecules and NCS ions. The

Table 2. Structural Parameters for the Solvated Lithium and Thiocyanate Ions in *Solution A*[a]

	p,q	r_{pq} / pm	b_{pq} / 10^2 pm^2	n_{pq}
$[Li(dmf)_6]^+$	Li–O	195(5)	0.5(2)	6[b]
	O–O	276[c]	2.0(5)	12[b]
	C···O	295(5)	3.0[c]	12[b]
	Li···C	280(5)	2.0[c]	6[b]
	Li···N	400(5)	3.0[c]	6[b]
	O···O	396[c]	3.0[c]	3[b]
	O···N	350[c]	3.0[c]	12[b]
	Li···C	460(8)	5.0[c]	12[b]
$[NCS(dmf)_n]^{n-1}$	S–O	380(5)	3.50(2)	1.55(4)
	S···C	380[c]	3.50(5)	1.55[c]
	S···N	430[c]	4.0[c]	3.1[c]
	S···C	480[c]	4.5[c]	3.1[c]
	S···C	550[c]	5.01[c]	3.1[c]

a) Uncertainties given in parentheses are probable values estimated from experimental errors. b) Fixed. c) Calculated from the varied bond lengths and frequency factors.

Table 3. Structural Parameters of the $[Mn(NCS)_4]^{2-}$ Complexes in *Solution B*[a]

	p,q	r_{pq} / pm	b_{pq} / 10^2 pm^2	n_{pq}
$[Mn(NCS)_4]^{2-}$	Mn–N(NCS)	220(5)	0.5(2)	4[b]
	Mn–C(NCS)	335[c]	2.0(5)	4[b]
	Mn–S(NCS)	500[c]	4.5(5)	4[b]
	N(NCS)···N(NCS)	359[c]	2.0(5)	6[b]
	N(NCS)···C(NCS)	458[c]	4.0[c]	6[b]
	N(NCS)···S(NCS)	609[c]	5.0[c]	6[b]
	C(NCS)···C(NCS)	547[c]	5.0[c]	6[b]

a) Uncertainties given in parentheses are probable values estimated from experimental errors. b) Fixed. c) Calculated from the varied bond lengths and frequency factors.

residual curve in the form of the difference radial distribution curve, $\{D(r)-4\pi r^2\rho_0\}_{res}$, is given in Fig. 4. In the LSQ fitting procedures r_{Li-X} (X=O, C, and N in DMF) and the temperature factors of the corresponding interatomic interactions were allowed to change. The remaining parameters were calculated from the geometry of the models. The octahedral model (R=0.06) resulted in far better fit than the tetrahedral one (R=0.14).

The small peak at about 200 pm in Fig. 4 indicated the Li–O interactions. Although the solvation number of the Li^+ ion was difficult to be estimated from the peak area, the position and the area of the second large peak around 280 pm were satisfactorily explained in terms of the octahedral structure of the solvated lithium ions. The tetrahedral model with the Li–O bond length of about 200 pm should have the O···O nonbonding interactions at about 330 pm as indicated by the broken line in Fig. 4. The shoulder (or a small peak) appearing at about 370 pm in the difference radial distribution curve could be explained in terms of the non-bonding O···N (about 350 pm) and *trans*-O···O (about 400 pm), as well as the Li···N (about 400 pm) interactions. As far as the temperature factors are concerned, only several of them were allowed to vary during the LSQ analysis, while most of them were fixed at reasonable values, determined by the value of the corresponding distances. The parameter values finally obtained for the solvated lithium ions were summarized in Table 2.

The repeated data analysis for *Solution* B resulted in a slightly longer Li–O bond length of 198 pm. Since *Solution B* contained more complicated species, more detailed discussion for the solvation structure of the lithium ion was not possible.

Solvation of the Thiocyanate Ion. Solvation of anions is usually so weak that reliable structural information can hardly be obtained. However, the number of the nearest neighbor solvent molecules of anions can be obtained by the solution X-ray diffraction method even though the solvent molecules are not strongly bound to the anions. Thiocyanate ions can certainly interact with DMF molecules in the solution. Since sulfur atom has a much larger scattering power than the other two atoms in the thiocyanate ion, interactions between the sulfur atom and atoms in the solvent molecules may become predominant in the structure function compared with other interatomic interactions in the solution. The bond length between the S atom in the thiocyanate ion and the O atom of the DMF molecule was varied in the course of the LSQ procedure. Atom-atom interactions between the thiocyanate ion and the DMF molecule other than the S–O pair were treated as dependent parameters calculable from the S–O pairs by assuming that the NCS^- ion (linear) and the DMF molecule (planar) are aligned parallel to their molecular axis. The results were summarized in Table 2. The average number of DMF molecules around the NCS^- ion was 3.1, and the S–O distance was estimated to be 380 pm. Since the contribution of the solvation structure of the thiocyanate ion to the total pair-correlation function (curve 3 in Fig. 2) was rather small compared with those from other atom pairs, the reliability of the structural parameters of the solvated thiocyanate ion given in Table 2 should be low. Nevertheless, introduction of the structural parameters of the solvated thiocyanate ion to the final result could improve the fit between theoretical and experimental $G(r)$ curves (see Fig. 2).

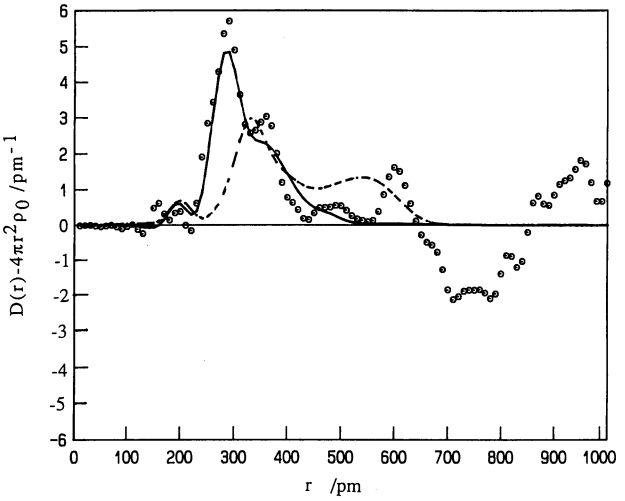

Fig. 4. Comparison between the experimental residual radial distribution function (circles) and the calculated ones from structural models of $[Li(dmf)_6]^+$ (full line) and $[Li(dmf)_4]^+$ (dashed line) in *Solution A*.

In the refinement of the structural parameters of *Solution B*, the average number of the nearest neighbor of solvent molecules around the thiocyanate ion was given to be 1.35, the uncertainty of the value, however, should be large.

Structure of the Tetrathiocyanato-*N*-manganate(II) Complex. The difference radial distribution curve for *Solution B* as shown in Fig. 5 was obtained by subtracting contributions of the solvent molecules, solvated lithium ions, and thioycanate ions by using the parameter values derived from *Solution A* from the total radial distribution function.

Three different geometrical models were tested in order to find the best fit structure of the tetrathiocyanatomanganate(II) complex in DMF: (i) the regular tetrahedral $[Mn(NCS)_4]^{2-}$, (ii) the octahedral $[Mn(NCS)_4(dmf)_2]^{2-}$ complex, in which the N atoms in the thiocyanate ions occupy the equatorial positions and the O atoms of DMF are at the axial positions, (iii) the tetragonal pyramidal $[Mn(NCS)_4(dmf)]^{2-}$ in which the O atom situates at the apex of the pyramid. In all of the models the molecular axis of the linear thiocyanate ions was assumed to direct towards the central metal ion, but the orientation of the solvating DMF molecules was not fixed in the course of the LSQ procedure. The

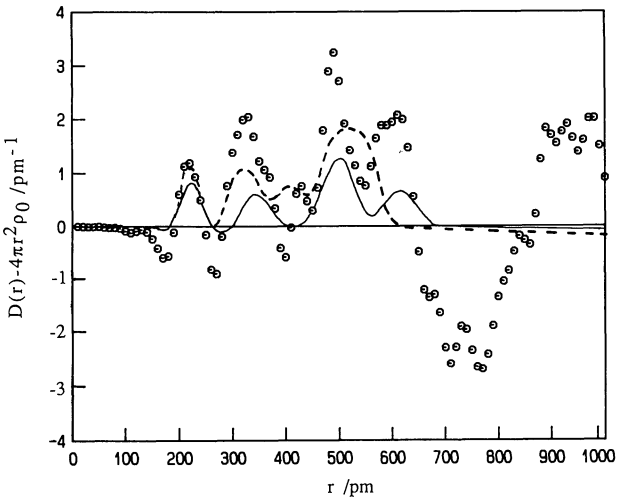

Fig. 5. Comparison between the experimental residual radial distribution function (circles) and the calculated ones from structural models of the octahedral $[Mn(NCS)_4(dmf)_2]^{2-}$ (dashed line) and the tetrahedral $[Mn(NCS)_4]^{2-}$ (full line) tetra-complexes in *Solution B*.

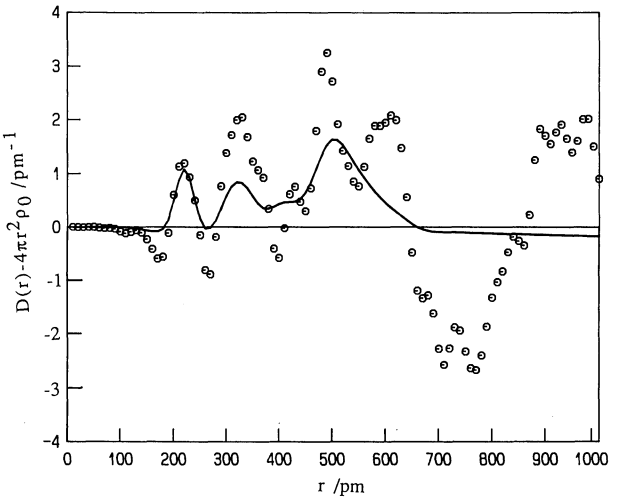

Fig. 6. Comparison between the experimental residual radial distribution function (circles) and the calculated ones from structural models of the 50 : 50% mixture of $[Mn(NCS)_4(dmf)_2]^{2-}$ and $[Mn(NCS)_3(dmf)_3]^-$ complexes (full line) in *Solution B*.

independent parameters were $r_{Mn-N(NCS)}$, r_{Mn-X}, (X=O, N, and C in the coordinated DMF molecules), and the temperature factors of the corresponding interactions. Other structural parameters were changed depending on the above independent parameters and the geometries assumed.

The LSQ calculations resulted in the *R*-factors of (i) 0.083, (ii) 0.078, and (iii) 0.081. Although the $\{D(r)-4\pi r^2\rho_0\}_{res}$ data scattered rather significantly due to subtraction of many contributions from the original curve, the modulation of the curve calculated from the octahedral model (the full line in Fig. 5) gave better fit to the residual curve than that from the tetrahedral model (the dashed line). The curve calculated from the model (iii) gave a line between the two. Thus, the best fit model among the three was concluded to be the octahedral $[Mn(NCS)_4(dmf)_2]^{2-}$ structure.

The structural parameters obtained as a result of the LSQ calculations were listed in Table 3. The distinction between Mn–O(dmf) and Mn–N(NCS) bonds was not possible in the course of the LSQ treatment, and we obtained the same bond length of them. The value of r_{Mn-O} and r_{Mn-N} of 220 pm was in good agreement with the value of r_{Mn-O}=219—222 pm found in aqueous solutions.[8—13]

However, according to equilibrium data of complex formation reactions of manganese(II) ions with thiocyanate ions in DMF,[4] *Solution B* should contain both dithiocyanatomanganese(II) and trithiocyanatomanganate(II) ions, together with the tetrathiocyanatomanganate(II) complex. A structural study on the $[Mn(NCS)_4]^{2-}$ by the calorimetric method suggested that the complex is tetra-coordinated.[4] Moreover, it seems that we do not have enough reason to exclude the possibility of the formation of the penta-coordinated $[Mn(NCS)_4(dmf)]^{2-}$ complex, or more plausibly, the coexistence of the tetra- and octahedral complexes with an equilibrium between $[Mn(NCS)_4]^{2-}$ and $[Mn(NCS)_4(dmf)_2]^{2-}$, because the *R*-factor determined for model (iii) was a value between the values for the models (i) and (ii).

Therefore, more careful analysis of the $s\cdot i(s)$ curve of *Solution B* should be necessary by taking into account the coexistence of the tri- and tetra-complexes with a tetrahedral or even a penta-coordinated trigonal bipyramidal structure together with the octahedral tetra-complex.

Structure of the Trithiocyanato-*N*-manganate(II) Complexes. Similar to the case discussed above, two different types of structure of the trithiocyanatomanganate(II) complex were examined, as if the complex were the only complex species in *Solution B*: (i) the octahedral $[Mn(NCS)_3(dmf)_3]^-$ and (ii) the tetrahedral $[Mn(NCS)_3(dmf)]^-$ structural forms. The *R*-factor at the LSQ fitting had its minimum again for the octahedral form with R=0.071, while the value was 0.084 for the case of (ii). The Mn–O and Mn–N bond lengths and the temperature factors of the atom-pairs were practically the same in the two models, and the different values of the *R*-factor in the two cases simply arise from the difference in the coordination numbers and the distances in the atom-pairs between the coordinated DMF molecules and thiocyanato ions in the first coordination shell of the manganese(II) ion.

From a preliminary analysis of the structure of the tri-complex, we concluded that the octahedral structure can be better accepted than the tetrahedral one, although a possibility of the latter structure could not be fully

excluded at that stage of the analysis. Formation of the dithiocyanatomanganese(II) complex was neglected in the course of the structural analysis because of its low concentration in *Solution B*.

In the final structural analysis combinations of possible structures discussed above were examined as follows: (i) The octahedral tri-complex $[Mn(NCS)_3(dmf)_3]^-$ + the tetrahedral tetra-complex $[Mn(NCS)_4]^{2-}$, (ii) the tetrahedral tri-complex $[Mn(NCS)_3(dmf)]^-$ + the tetrahedral tetra-complex $[Mn(NCS)_4]^{2-}$, (iii) the octahedral tri-complex $[Mn(NCS)_3(dmf)_3]^-$ + the octahedral tetracomplex, $[Mn(NCS)_4(dmf)_2]^-$ (iv) (50% octahedral $[Mn(NCS)_3(dmf)_3]^-$ + 50% tetrahedral $[Mn(NCS)_3(dmf)]^-$ tri-complex) + the tetrahedral tetra-complex $[Mn(NCS)_4]^{2-}$.

The case of tetrahedral tri-complex + octahedral tetra-complex was excluded because it may be unexpected that the structure of complexes of consecutive steps change twice when the ligand number increases. During the analysis, the ratio in percentage between the pairs of complexes was varied.

Figure 7 shows the *R*-factors for cases (i) and (ii). Cases (iii) and (iv) could immediately be excluded, since the *R*-factor was lowered only when a negative coordination number was supposed. Finally, the absolute minimum of *R*-factor was reached for case (ii), and when the supposed distribution of the tri- and tetra-complexes was 50 : 50%.

Table 4 lists the structural parameters for the octahedral trithiocyanato complex.

This result can be well understood qualitatively if we observe the peak shapes shown in Fig. 5 in forms of $\{D(r)-4\pi r^2\rho_0\}_{res}$ with the change in the fraction of the tetra-complex. The contributions arising from tetrahedral complexes will fit better to the small peak at 220 pm and reflect better the overall shape of the residual curve, but they cannot supply enough contribution to fit. The octahedral arrangement requires more DMF molecules to be involved into the first neighbor structure

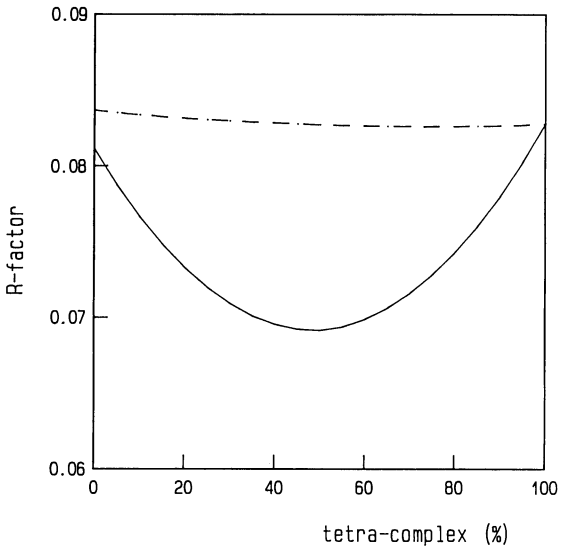

Fig. 7. The variation of the Hamilton *R*-factor values as a function of distribution of the tri- and tetrathiocyanatomanganate(II) complexes (in percent of the tetra-complex). Full line: the octahedral tri-complex $[Mn(NCS)_3(dmf)_3]^-$ + the tetrahedral tetra-complex $[Mn(NCS)_4]^{2-}$ (case i), dashed line: the tetrahedral tri-complex $[Mn(NCS)_3(dmf)]^-$ + the tetrahedral tetra-complex $[Mn(NCS)_4]^{2-}$ (case ii).

Table 4. Structural Parameters of the $[Mn(NCS)_3(dmf)_3]^-$ Complexes in *Solution B*[a)]

	p,*q*	r_{pq} / pm	b_{pq} / 10^2 pm^2	n_{pq}
$[Mn(NCS)_3(dmf)_3]^-$	Mn–O(dmf)	220(5)	0.5(2)	3[b)]
	Mn–N(NCS)	220(5)	0.5(2)	3[b)]
	Mn···C(NCS)	335[c)]	2.0(5)	3[b)]
	Mn···S(NCS)	500[c)]	4.5(5)	3[b)]
	Mn···C(dmf)	301(7)	1.8(5)	3[b)]
	Mn···N(dmf)	414(8)	3.0[c)]	3[b)]
	Mn···C(dmf)	435(8)	3.0[c)]	3[b)]
	Mn···C(dmf)	536(8)	4.5[c)]	3[b)]
	O(dmf)···N(NCS)	311[c)]	2.0(2)	6[b)]
	N(NCS)···N(NCS)	311[c)]	2.0(5)	3[b)]
	O(dmf)···C(NCS)	401[c)]	3.0[c)]	6[b)]
	N(NCS)···C(NCS)	401[c)]	3.0[c)]	6[b)]
	N(NCS)···S(NCS)	546[c)]	5.0[c)]	6[b)]
	C(NCS)···S(NCS)	474[c)]	4.0[c)]	6[b)]
	O(dmf)···S(NCS)	546[c)]	5.0[c)]	6[b)]
	C(NCS)···C(NCS)	474[c)]	4.0[c)]	3[b)]
	O(dmf)–O(dmf)	301[c)]	2.0(5)	6[b)]
	O(dmf)–N(NCS)	440[c)]	3.5[c)]	3[b)]
	O(dmf)–C(NCS)	555[c)]	5.0[c)]	3[b)]

a) Uncertainties given in parentheses are probable values estimated from experimental errors. b) Fixed. c) Calculated from the varied bond lengths and frequency factors.

of the Mn^{2+} ions with increasing number of contributions in the 300—320 and 400—480 region. The best fit is then a compromise between the two sets of contributions.

Our result is in full agreement with the findings of the previous calorimetric measurements that the dominating species for the tetra-complexes has tetrahedral structure, while the tri-complex seems to be octahedral. The minimum of the *R*-factors was produced at a somewhat different distribution of the tri- and tetra-complexes from what is estimated from the stability constants. We would emphasize, that the main result of our study is that a distinction of octahedral and tetrahedral complexes could be made, in consistency with the suggestion derived from calorimetric data. Moreover, our results also support the conclusion that the structural change should occur at the fourth step rather than at the third one of the ligand build up.

The work has been financially supported, in part, by the Grant-in-Aid for Scientific Research on Priority Area of "Molecular Approaches to Non-Equilibrium Processes in Solution" from the Ministry of Education, Science and Culture, (No. 03245106). One of us (TR) is greatly indebted to the Institute for Molecular Science and the Hungarian Academy of Sciences for establishing the conditions of the common work.

References

1) T. Yamaguchi, K. Yamamoto, and H. Ohtaki, *Bull. Chem. Soc. Jpn.*, **58**, 3235 (1985).

2) I. Persson, A. Iverfeldt, and S. Ahrland, *Acta Chem. Scand., Ser. A*, **35**, 295 (1981).

3) K. Ozutsumi, T. Takamuku, S. Ishiguro, and H. Ohtaki, *Bull. Chem. Soc. Jpn.*, **62**, 1875 (1989).

4) S. Ishiguro and K. Ozutsumi, *Inorg. Chem.*, **29**, 1117 (1990).

5) G. Kabisch, E. Kálmán, G. Pálinkás, T. Radnai, and F. Gaizer, *Chem. Phys. Lett.*, **107**, 463 (1984).

6) H. Ohtaki, S. Itoh, T. Yamaguchi, S. Ishiguro, and B. M. Rode, *Bull. Chem. Soc. Jpn.*, **56**, 3406 (1983).

7) T. Radnai, S. Itoh, and H. Ohtaki, *Bull. Chem. Soc. Jpn.*, **61**, 3645 (1988).

8) M. Cannas, G. Carta, A. Cristini, and G. Marongiu, *J. Chem. Soc., Dalton Trans.*, **1976**, 300.

9) L. A. Aslanov, V. M. Zonov, and K. Kynev, *Sov. Phys. Crystallogr.*, **21**, 693 (1976).

10) H. Ohtaki, T. Yamaguchi, and M. Maeda, *Bull. Chem. Soc. Jpn.*, **49**, 701 (1976).

11) R. Caminiti, G. Marongiu, and G. Paschina, *Z. Naturforsch., A*, **37**, 581 (1982).

12) G. Licheri, G. Paschina, G. Piccalugga, and G. Pinna, *J. Chem. Phys.*, **81**, 6059 (1984).

13) R. Caminiti, P. Cucca, and T. Pintori, *Chem. Phys.*, **88**, 155 (1984).